Inductor Design Optimization Using FEA Supervised Machine Learning

D. Cajander[1,3], I. Viarouge[2], P. Viarouge[3], D. Aguglia[3,4]

[1]ENERGY Inst., Haute Ecole d'Ingénieurie et d'Architecture Fribourg, HES-SO University of Applied Sciences and Arts Western Switzerland, Boulevard de Pérolles 80
CH-1700 Fribourg, Switzerland
Tel. : +41 26 429 65 57
Email: david.cajander@hefr.ch
https://www.heia-fr.ch

[2] ELECTROTECHNOLOGIES Selem Inc, 2610, Rue Gérard-Lajoie, GIP 3G1, Quebec (QC), Canada
Email: selem@oricom.ca

[3]LEEPCI Lab., Electrical and Computer Eng. Dept., Laval University, GIK 7P4, Quebec (QC), Canada
Email: philippe.viarouge@gel.ulaval.ca

[4]CERN - European Organization for Nuclear Research, Accelerator Systems Dept., Electric Power Converter Group
CH- 1211 Geneva 23, Switzerland
Email: davide.aguglia@cern.ch

Acknowledgements

DC thanks Beat Wolf[5] for his collaboration on data analysis and machine learning ([5]Institute of Complex Systems, Haute Ecole d'Ingénieurie et d'Architecture Fribourg, HES-SO University of Applied Sciences and Arts Western Switzerland, Boulevard de Pérolles 80, CH-1700 Fribourg, Switzerland).

Keywords

«Magnetic device», «Machine learning», «Deep Learning», «Design optimization», «Finite-element analysis», «Data analysis», «Neural network», «Passive component»

Abstract

An optimal inductor design methodology using dimensioning models derived from Finite Element Analysis (FEA) supervised Artificial Neural Networks (ANN) is presented. The efficiency of such trained ANN dimensioning models in terms of compromise between precision and computing time is demonstrated for the cylindrical inductor topology with air and magnetic material core including saturation.

Introduction

Inductors are widely used in all kinds of power converters like SVC, AFE, and Multilevel Converters for energy storage, AC & DC filtering and magnetic coupling functionalities. Such magnetic components are often specified by the power electronics engineer considering them as simple elements of an electrical circuit. However, their practical feasibility, size, thermal or electro-mechanical (e.g. short circuits) behaviors can easily be overlooked. In the more and more demanding quest for compact and economical solutions, these aspects shall be carefully considered since the early steps of the converter

design. For each application, inductors are subject to several requirements, such as electrical insulation, thermal and mechanical aspects, inductance linearity over a specified current range, internal resistance, fault currents to withstand, and lifetime [2]. The inductor design is a multi-variable non-linear optimization problem where the performance objectives to minimize are the volume and/or the mass and the cost. Several constraints can also be defined depending on the requirements. Several different inductor topologies presented in Fig. 1 can be evaluated by the designer to make an optimal choice for each application. A versatile and generic design methodology is mandatory.

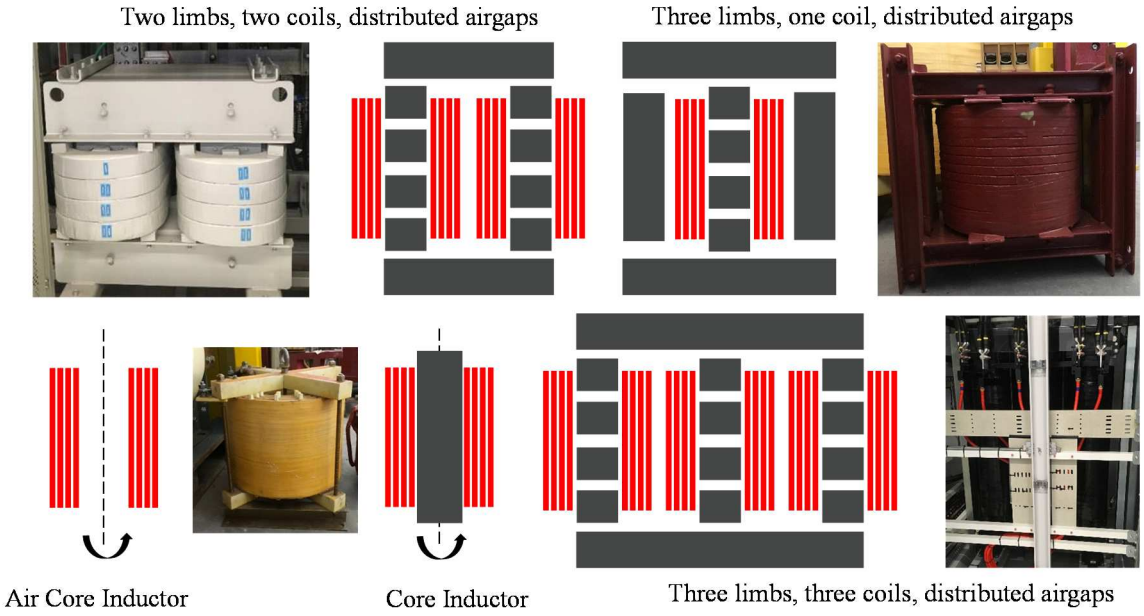

Fig. 1: Main inductor topologies used in Power Converters

Cylindrical Inductor topologies and application

The FEA supervised ANNs optimal design methodology presented in this paper has been applied to the following cylindrical inductor topologies: the cylindrical air core inductors and the cylindrical inductors with a magnetic core as shown in Fig.2. These kinds of inductors are used in several AC & DC filtering applications like the air core inductors used in SVC with thyristor-controlled reactor (TCR).

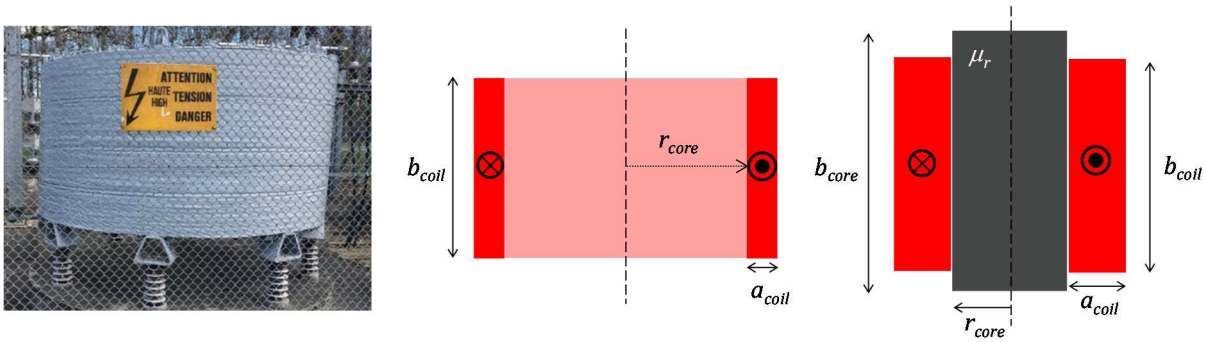

Fig. 2: Cylindrical air core inductor used in SVC with thyristor-controlled reactor (TCR) and Cylindrical inductor with magnetic material core

Cylindrical Inductor Design Optimization Using FEA

The inductor CAD environment is presented in Fig. 3. The optimal design methodology is using an inverse problem approach where a Non-Linear Optimization procedure (NLO) is associated to a device dimensioning model to minimize an objective function while respecting the specification constraints.

There are three different components in the dimensioning model: an electromagnetic model, a thermal model and a mechanical model.

In this modular CAD environment, the user can choose models with different levels of complexity according to a suitable compromise between accuracy and computing time. For example, in the electromagnetic dimensioning model, the inductance can be computed by a simplified analytical model [1] or a complex model based on 2D or 3D Finite Element Analysis (FEA) including non-linear B(H) characteristics of the core magnetic material.

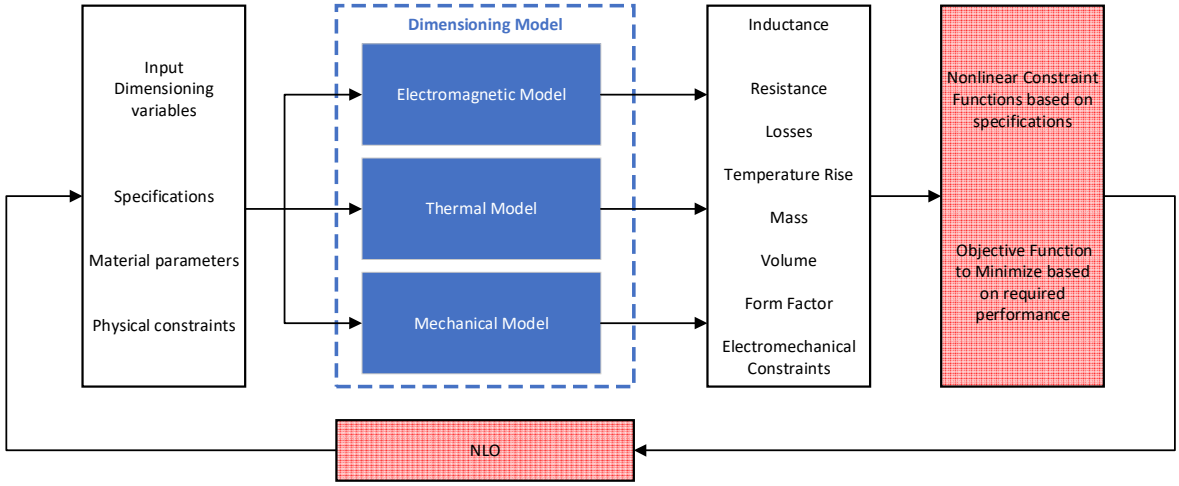

Fig. 3: Cylindrical inductor optimal design environment

Input dimensioning variables

There are 3 independent geometric dimensions for the air core inductor and 4 independent geometric dimensions for the magnetic core inductor as shown in Fig. 2.
By introduction of dimensionless form factors, the geometric variables can be naturally scaled to the coil inner radius r_{core} (m):

$$FF_{a_{coil}/r_{core}} = \frac{a_{coil}}{r_{core}} \qquad FF_{b_{coil}/r_{core}} = \frac{b_{coil}}{r_{core}} \qquad FF_{b_{core}/b_{coil}} = \frac{b_{core}}{b_{coil}} \tag{1}$$

It has been shown that the use of dimensionless form factors is providing an efficient preliminary scaling to improve the NLO method efficiency.
There are 5 independent dimensioning variables for the optimal air core inductor design problem: 3 geometric dimensions, the number of turns *N* and the current usually imposed by the specifications.
There are 6 independent dimensioning variables for the optimal magnetic core inductor design problem: 4 geometric dimensions, the number of turns *N* and the current usually imposed by the specifications.

Objective function of the optimization method

Several objective functions can be used in the environment but the usual function to minimize during the cylindrical inductor design is the mass of the copper coil or the total mass of the core and the coil. The value of the objective function to minimize is computed from the input variables by use of the mechanical dimensioning model at each iteration of the optimization process.

Constraint functions of the optimization method

The constraint functions of the design optimization problem are directly derived from the main inductor specifications like the required inductance value, the peak and RMS current, the inductance linearity over a specified current range in the case of a saturable magnetic core inductor, the DC resistance, the quality factor in AC applications, the ambient temperature, the maximum temperature rise, the electrical isolation specs and the overall dimensions or space constraints. As shown in Figure 3, the values of the

different constraint functions are computed from the input variables by use of the electromagnetic, thermal and mechanical dimensioning models at each iteration of the optimization process.

Electromagnetic dimensioning model

The main challenge in the dimensioning models used in the optimal design environment is the accuracy of the inductance computation for each set of the input variables. In order to meet the requirements with these inductor topologies, the inductance must be computed by a model based on Finite Element Analysis (FEA). According to their cylindrical symmetry, a 2D Finite Element Analysis (FEA) is preferred. With such a method, the non-linear characteristic B(H) of the core magnetic material can also be taken into consideration in the case of a saturable magnetic core inductor. Depending on the specified inductance linearity over the imposed current range and on the characteristics of the magnetic material in use, it is also possible in some applications to consider that the material relative permeability μ_r is constant over the specified current range.

In the case of the cylindrical air core inductor, the inductance to be computed by 2D FEA at each iteration of the NLO process is independent of the current and a function of 4 input variables only:

$$L = N^2 . L_1(r_{core}, FF_{a_{coil}/r_{core}}, FF_{b_{coil}/r_{core}}) \quad (2)$$

In this case, the specific or one-turn inductance (N=1) L_1 is a function of 3 variables only.

In the case of a cylindrical inductor with a magnetic material core of fixed linear relative permeability μ_r, the inductance to be computed by 2D FEA at each iteration of the NLO process is independent of the current and a function of 5 input variables:

$$L = N^2 . L_1(r_{core}, FF_{a_{coil}/r_{core}}, FF_{b_{coil}/r_{core}}, FF_{b_{core}/b_{coil}}) \quad (3)$$

In this case, the specific or one-turn inductance (N=1) L_1 is a function of 4 variables only.

In the case of the cylindrical inductor with a core made of saturable magnetic material with a non-linear characteristic B(H), the inductance to be computed by 2D FEA at each iteration of the NLO process is dependent of the current density and a function 6 input variables:

$$L = N^2 . L_1(r_{core}, FF_{a_{coil}/r_{core}}, FF_{b_{coil}/r_{core}}, FF_{b_{core}/b_{coil}}, J) \quad (4)$$

One can notice that for a fixed number of turns N, the product of the current density J (A/m^2) by the copper coil section imposed by the geometric dimensions is equal to the total coil magnetomotive force MMF. This MMF and the geometric dimensions are then fixing the magnetic field H distribution and consequently the core induction B distribution through the core according to the magnetic material characteristic $B(H)$.

In this case, the specific or one-turn inductance (N=1) L_1 is a function 5 variables only.

Non-Linear Optimization procedure (NLO)

The NLO procedure used in the cylindrical inductor optimal design environment presented in Fig. 3 is the Generalized Reduced Gradient (GRG) method [13].

Air core optimal design example using FEA

An application example of the optimal design methodology is illustrated in Fig. 4 in the case of a specified 10mH 100A air core inductor with 95°C temp rise. The objective function is the coil mass minimization. The convergence and precision characteristics of the NLO process are detailed in Table I. At each iteration of the NLO process, the mass, the losses, the resistance and the temperature rise are derived from the thermal and mechanical dimensioning models and the inductance is computed by 2D FEA. One can notice the number of iterations of the GRG method that is needed to converge towards the optimal solution. The inductance computation by the 2D FEA at each iteration is slowing the execution time.

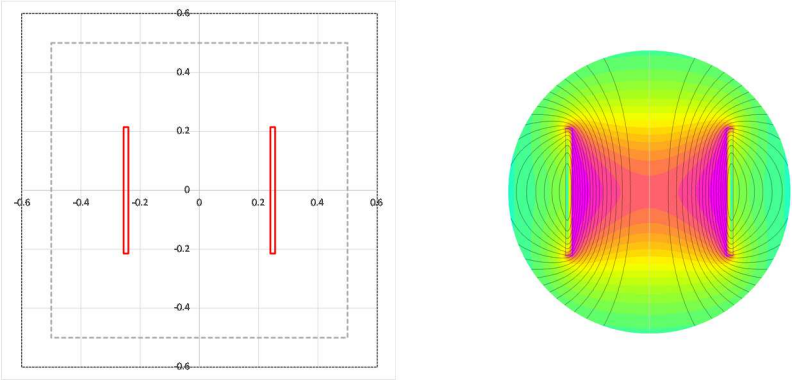

Fig. 4: Application example of FEA optimal design: 10mH 100A Cylindrical air core inductor with 95°C temp rise (r_{core}= .225m, $FF_{a_{coil}/r_{core}}$ = .0904 , $FF_{b_{coil}/r_{core}}$= 1.6463 , N=165)

Table I: Air core inductor optimization example using FEA

Air core inductor	Specifications		Optimal solution			NLO process	
Inductance (H)	Current (A)	Temp Rise (°C)	Copper Mass (kg)	Inductance (H)	Relative error to specs (%)	GRG Iterations number	Execution time (s)
1.00E-02	100	95	99.9	9.76E-03	2.4	1115	239

This example demonstrates that despite their better performance in terms of precision, the FEA techniques can become heavy and time consuming in an iterative optimization process. Hybrid methods like space mapping techniques combining coarse and fine models in the same optimization process have been proposed in the literature [3][4] to reach a feasible optimal solution with a limited number of finite element computations. This solution is validated by FEA with a suitable compromise between precision and computing time but its unicity and optimality are not guaranteed [5]. In this paper, another alternative is investigated to solve the preceding compromise by using the accurate FEA method to train Artificial Neural Networks (ANNs) dimensioning models and improve the computing and convergence efficiency of the NLO method [6] [7].

Supervised Artificial Neural Networks (ANNs) Dimensioning Models

Artificial Neural Networks (ANNs) are fast becoming a new viable approach to replace FEA based dimensioning models for optimal design, thanks to their gain in computing speed and simplicity. For instance, pre-trained ANN models are essentially smooth functions of tuned parameters, thus, the gradient is readily computed exactly compared to FEA methods. The ANN approach can been extended to saturated core inductors [8] [9] because it is possible to train and build a neural network to model nonlinear relationship by a suitable choice of the neural network architecture, the learning rate, the learning algorithm and the activation function.

In this paper, the ANNs or models are trained in a supervised setting and their creation is following the associated typical workflow described in Fig. 6. In the supervised setting, a model is trained on a dedicated database of labeled input/target pairs to minimize the error between its predictions computed from the inputs and the associated targets, in this case inductances [11].

Generation of inductance databases with FEA

Three databases presented in Table II and Table III have been generated from 2D FEA magnetostatic computation of specific inductances L_1 (N=1) using the FEA tool integrated in the inductor CAD environment of Fig. 3: Database 1 for cylindrical air core inductors, Database 2 for cylindrical inductors with a magnetic material core of fixed linear relative permeability μ_r =1000, Database 3 for cylindrical inductors with a magnetic core made of saturable material presenting a non-linear characteristic *B(H)*.

In Database 3, the range and distribution of the current density J is adjusted for each set of dimensions and form factors in order to operate the core magnetic material on its whole *B(H)* nonlinear range (the product of J by the copper coil section imposed by the dimensions is equal to the total coil magnetomotive force that is fixing the core induction level B irrespective of the turn number). This approach is illustrated in Fig. 5 by the $L_1(J)$ and $B(J)$ characteristics of one inductor of Database 3 with a given set of dimensions and form factors.

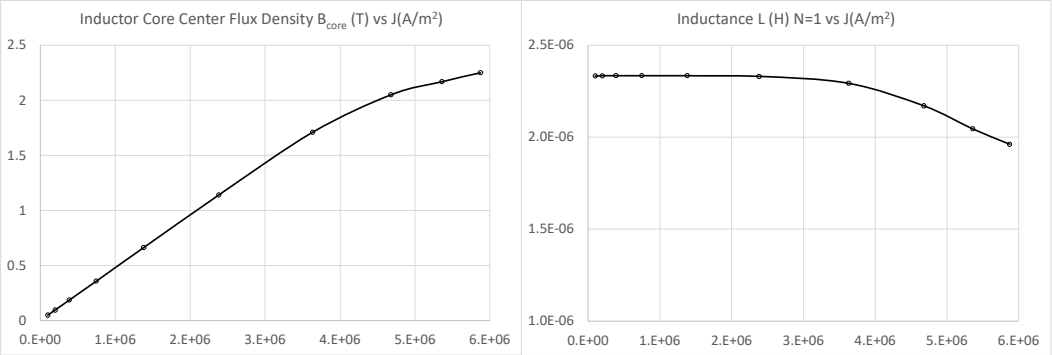

Fig. 5: Non-linear $L_1(J)$ and $B(J)$ characteristics of one specific inductance L_1 of Database 3 with a given set of dimensions & form factors (M19 core magnetic material used)

Table II: Inductance Databases for Supervised learning models

Inductor Database	Output: specific or one-turn inductance (N=1) computed by FEA	Number of inputs	Number of samples & Generation time
Database 1 Air core inductor	$L_1(r_{core}, FF_{a_{coil}/r_{core}}, FF_{b_{coil}/r_{core}})$	3	125000 8h 18 mn
Database 2 Magnetic core inductor with fixed permeability material μ_r=1000	$L_1(r_{core}, FF_{a_{coil}/r_{core}}, FF_{b_{coil}/r_{core}}, FF_{b_{core}/b_{coil}})$	4	104976 7h 23mn
Database 3 Saturable core inductor with M19 Laminated Silicon Steel	$L_1(r_{core}, FF_{a_{coil}/r_{core}}, FF_{b_{coil}/r_{core}}, FF_{b_{core}/b_{coil}}, J)$	5	190080 19h 33mn

Table III: Database variables mean and standard deviation

Database	r_{core} (m)		$FF_{a_{coil}/r_{core}}$		$FF_{b_{coil}/r_{core}}$	
	Mean	Std	Mean	Std	Mean	Std
Database 1	0.395	0.119	1.235	0.432	1.235	0.432
Database 2	0.400	0.111	1.208	0.432	1.208	0.432
Database 3	1.411	0.460	1.187	0.431	1.187	0.431

Database	$FF_{b_{core}/b_{coil}}$		J (A/m^2)		L_1 (H)	
	Mean	Std	Mean	Std	Mean	Std
Database 1	--	--	--	--	1.00E-06	3.50E-07
Database 2	0.761	0.403	not applicable	not applicable	1.50E-05	5.30E-06
Database 3	1.458	0.287	8.70E+05	9.40E+05	7.00E-06	2.00E-06

Workflow of ANN supervised training

The workflow for creating a model starts with the preprocessing of the database (see Tables II & III for the details of the database used). It is more efficient to train ANNs when the inputs and targets are all scaled to be in the interval [0, 1]. Thus, the inputs were standardized by computing their z-scores and a logarithm was applied to the target air core inductors and the magnetic core inductors with fixed permeability material of Database 1&2. The preprocessing for the database of saturable core inductors (Database 3) is slightly different: instead of applying a logarithm to the target inductances, a Z-standardization was applied similarly to the inputs.

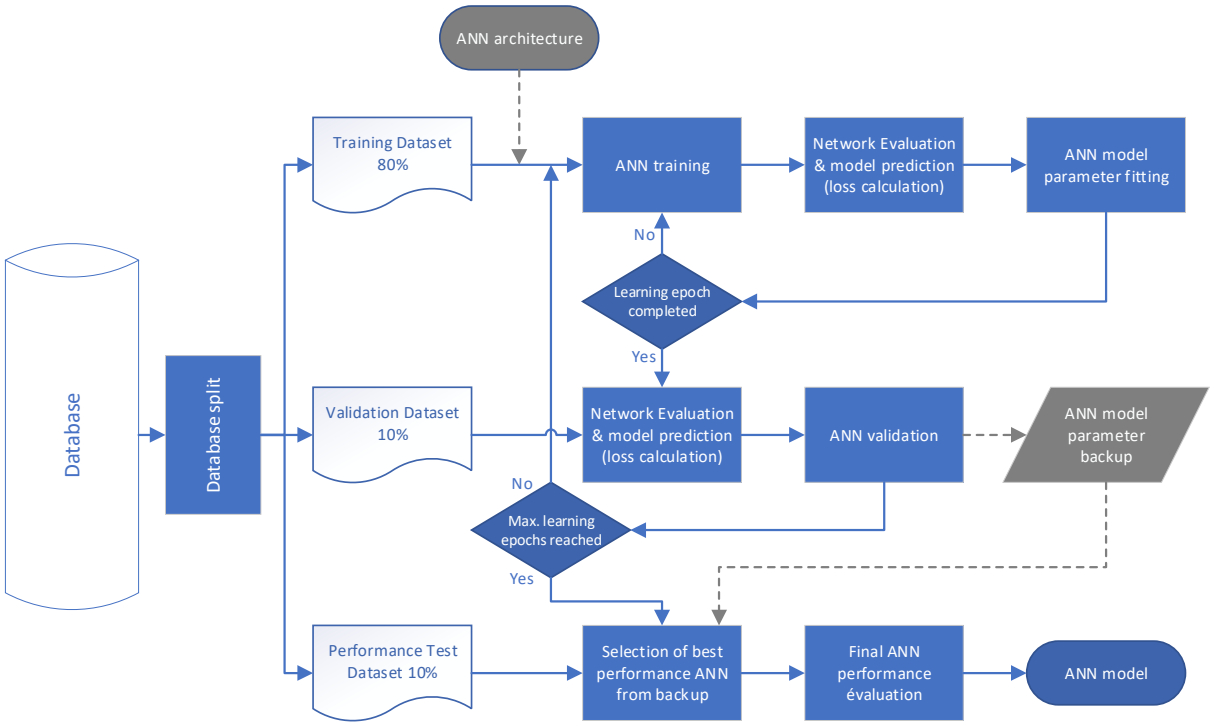

Fig. 6: Workflow of ANN supervised training

Before training, the database is shuffled and divided into 3 subsets: a training set (80%), a validation set (10%) and an evaluation set (10%).

During the training stage, the model predicts the inductance of all the training set inputs, then the error between the predictions and the targets is evaluated using a loss function, finally the parameters of the model are updated through a gradient descent algorithm relying on backpropagation to compute the gradient of the parameters [11]. One training iteration or epoch is completed after all the labeled pairs in the training set have been explored. In this paper, the mean squared error between prediction and target was used as the loss function. The first models were trained for 100 epochs and the third model for 500 epochs.

While training is underway, the performance of the model is evaluated using the validation set to identify overfitting on new data at a set interval of epochs. The loss is computed using the same loss function used on the training set. A backup of the model is created.

After the set number of epochs is reached, the models that were saved during validation are evaluated on the evaluation set composed of data unseen during training. The best performing model is then selected as the final model.

Parameters pertaining to model architecture such as number of layers, number of neurons per layer and the learning rate, must be specified before training and will be kept fixed thereafter. In this article, these hyper-parameters were optimized using the Optuna [12] framework and the machine learning was handled using the Pytorch [10] library.

ANN Architecture and Learning Optimization

In order to enhance the general performance of an ANN, it is important to determine the best network architecture and learning rate. Therefore, the ANN architecture optimization is done ahead of the training in a separate cycle of trials. The process starts with a random set of hyperparameters that are each comprised in predefined ranges set by the user (i.e. number of layers, number of hidden neurons and the learning rate). After a training cycle of 20 epochs the performance and the hyperparameters are stored and a new trial is started with a different set of hyperparameters. The Optuna framework determines the next hyperparameters to be tested based on the performance of the past recorded trials. This iterative process allows to refine the ANN architecture and learning rate according to the latest results. After a series of 100 trials, each made of 20 training epochs, the best performing ANN hyperparameters are stored to allow the training process to start directly with an optimized set of hyperparameters. This enhances the learning and forecasting abilities of the ANN model, while reducing the training effort for a given performance as well.

Description of the three Trained ANNs

The architecture of the three trained models and their performance on their test set are reported in table IV. Every model is a fully connected ANN whose activation function after every hidden layer is the Rectified Linear Unit (ReLu). The architecture of Model 1 is illustrated in Fig. 7.

Table IV: Test Set Performance of the Trained Models

	Database	Number of Inputs	Number of Hidden layers	Number of neurons per layer	Average Absolute error	Min Absolute error	Max Absolute error
Model 1 Air core inductor	**Database 1**	3	2	396	1.147e-08	1.085e-13	4.826e-07
Model 2 Magnetic core inductor μ_r=1000	**Database 2**	4	3	162	5.441e-09	1.054e-15	4.550e-08
Model 3 Saturable core inductor	**Database 3**	5	5	400	1.226e-07	3.183e-12	8.771e-07

All models are trained with a mini-batch gradient descent and the optimizer was Pytorch's Adam with an optimal learning rate according to the described learning optimization method. Model 1 and 2 were trained in 100 epochs while Model 3 was for 500 epochs. The reported models were the best ones found during training with the smallest validation loss.

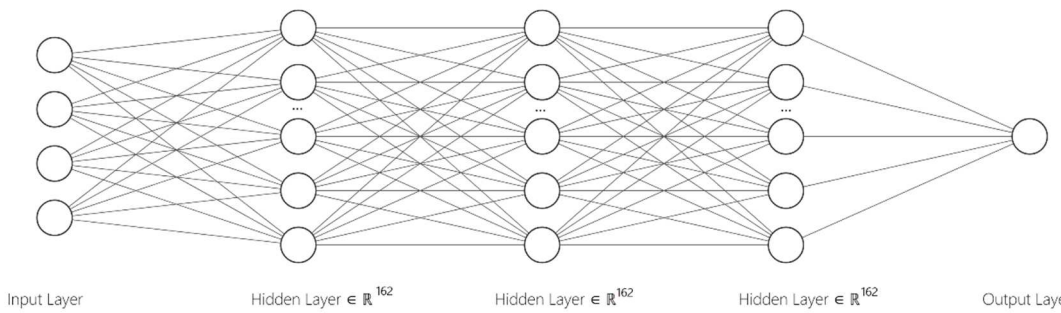

Fig. 7: Architecture of the fully-connected ANN Model 1

Cylindrical Inductor Design Optimization Using ANNs

The three ANN Models have been integrated in the inductor CAD environment of Fig. 3 to be used for the optimal design of the three kinds of cylindrical inductors: air core type (Model 1), magnetic core type with constant μ_r=1000 (Model 2), saturable magnetic core type (Model 3). At each iteration of the NLO process, the mass, the losses, the resistance and the temperature rise are still derived from the thermal and mechanical dimensioning models but the inductance is no longer computed from 2D FEA but from one of the trained ANN model. Three specific examples are presented to validate the proposed optimal inductor design methodology using supervised ANNs and to compare its performance to the optimal inductor design methodology using the direct FEA approach that was presented in the first part of this paper. In order to precisely quantify the relative performances of both methods, the initial guess of the NLO process are identical.

Air core optimal design example

Table V presents the comparative analysis of both optimal design methodologies in the case of the same 10mH 100A air core inductor with 95°C temp rise of Table I and Figure 4. The same objective and constraint functions are used. The dimensions of both optimal solutions are very close r_{core}= 0.239m vs .225m , $FF_{a_{coil}/r_{core}}$= 0.067 vs .0904, $FF_{b_{coil}/r_{core}}$= 1.7902 vs 1.6463, N=170 vs 165. The comparative analysis of the optimal solutions found in terms of optimal mass, relative error, convergence and precision characteristics of the NLO process are detailed in Table V. The number of iterations of the GRG algorithm is 9% lower with the ANN Model 1. The computation time of the NLO process with the use of the ANN Model 1 is 66 times faster than with the direct use of FEA.

Table V: FEA vs ANN Optimization for an air core inductor

	Specifications					Optimal solution	
	Inductance (H)	Current (A)	Copper Mass (kg)	Inductance (H)	Relative error to specs (%)	Iterations number	Execution time (s)
Optimization with FEA	1.00E-02	100	99.9	9.76E-03	2.4	1115	239
Optimization with ANN Model 1	1.00E-02	100	96.3	9.99E-03	0.1	1020	3.6

Constant permeability magnetic core inductor optimal design example

Table VI and Fig. 8 present the comparative analysis of both optimal design methodologies in the case of a 10mH 100A magnetic core inductor with μ_r=1000 and 95°C temp rise. The objective function is the total mass minimization. The comparative analysis of the optimal solutions found in terms of optimal mass, relative error, convergence and precision characteristics of the NLO process are detailed in Table VI. The number of iterations of the GRG algorithm is 23% lower with the ANN Model 2. The computation time of the NLO process with the use of the ANN Model 2 is 54 times faster than with the direct use of FEA.

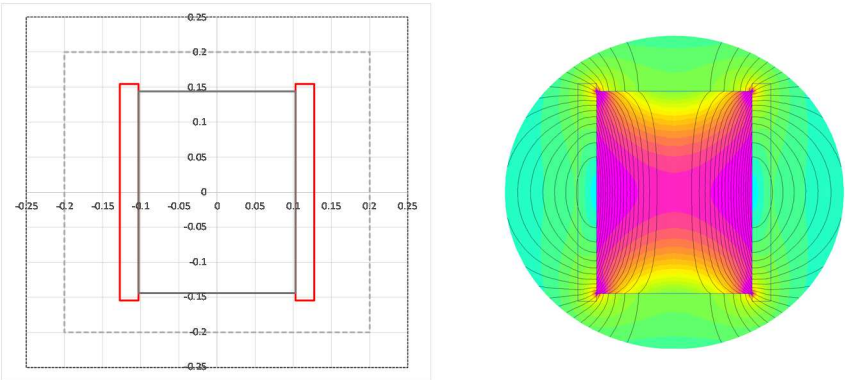

Fig. 8: Cylindrical inductor Magnetic core inductor with constant permeability (dimensions in m)

Table VI: FEA vs ANN Optimization for a magnetic core inductor with μr=1000

	Specifications					Optimal solution	
	Inductance (H)	Current (A)	Total Mass (kg)	Inductance (H)	Relative error to specs (%)	Iterations number	Execution time (s)
Optimization with FEA	1.00E-02	100	106.8	9.68E-03	3.2	1206	155
Optimization with ANN Model 2	1.00E-02	100	119.2	9.99E-03	0.1	930	2.85

Saturable magnetic core inductor optimal design example

Table VII and Fig. 9 present the comparative analysis of both optimal design methodologies in the case of a 44.8mH 100A saturable magnetic core made of M19 Laminated Silicon Steel inductor with 95°C temp rise. The objective function is the copper mass minimization in this example. The comparative analysis of the optimal solutions found in terms of optimal copper mass, relative error, convergence and precision characteristics of the NLO process are detailed in Table VII. The number of iterations of the GRG algorithm is 7% higher with the ANN Model 3. The computation time of the NLO process with the use of the ANN Model 3 is 214 times faster than with the direct use of FEA.

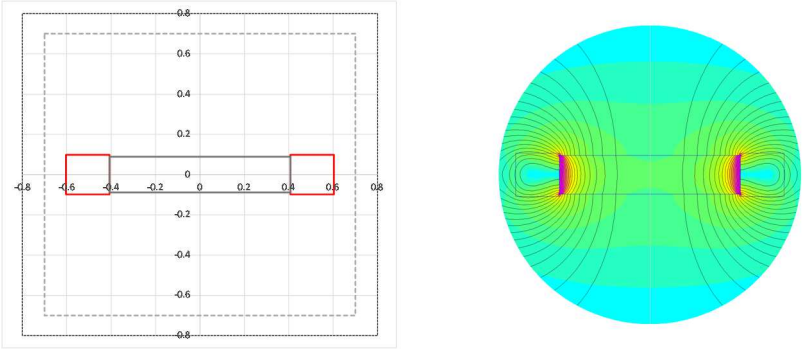

Fig. 9: Cylindrical inductor with a saturable magnetic core inductor including non-linear material B(H) characteristic (dimensions in m)

Table VII: FEA vs ANN Optimization for a saturable magnetic core inductor

	Specifications		Optimal solution			NLO process	
	Inductance (H)	Current (A)	Copper Mass (kg)	Inductance (H)	Relative error to specs (%)	Iterations number	Execution time (s)
Optimization with FEA	4.48E-02	100	925	4.62E-02	3.0	2496	1872
Optimization with ANN Model 3	4.48E-02	100	1092	4.51E-02	0.5	2676	8.76

One can notice in the three examples that the precision of the ANN models is highly acceptable for inductor design purpose. The number of GRG iterations is usually lower with the ANN model for a better relative precision. The ANN model inductance computation time is 54 to 66 times faster than in the FEA case without saturation. In the case of a saturable inductor nonlinear FEA become heavy and time consuming and the ANN model inductance computation time is 214 times faster. FEA supervised Artificial Neural Networks dimensioning models can replace the time consuming FEA method with the same accuracy in the optimal design environment and highly improve the computing and convergence efficiency of the NLO method.

Conclusion

It has been clearly demonstrated on this example of inductance topology that the use of FEA supervised trained ANNs dimensioning models is a very efficient alternative in terms of compromise between precision and computing time in an optimal inductor design environment. The systematic use of dimensionless form factors as input variables of the supervised ANN model also provides inherent preliminary scaling that improve the convergence of the training process. This methodology can be efficiently extended to the optimal design of the other inductor topologies presented in Fig. 1 and to other parts of the dimensioning model used in the environment like the computation of electro-magnetic forces or the heavy FEA computations of HF copper losses in AC applications.

References

[1] H. A. Wheeler: Formulas for the Skin Effect, Proceedings of the IRE, vol. 30, no. 9, pp. 412-424, Sept. 1942, doi: 10.1109/JRPROC.1942.232015.

[2] Sudhoff S. D.: Introduction to Inductor Design, Power Magnetic Devices: A Multi-Objective Design Approach, Wiley- IEEE Book Chapter, 2022,

[3] Choi H.-S. et al.: A new design technique of magnetic systems using space mapping algorithm, IEEE Transactions on Magnetics, Vol 37, no 5, p 3627 3630

[4] Leal-Romo F. et al.: Design optimization of a planar spiral inductor using space mapping, IEEE 26th Conference on Electrical Performance of Electronic Packaging and Systems (EPEPS), 2017, 3 p.

[5] S. Candolfi, P. Viarouge, D. Aguglia and J. Cros: Hybrid design optimization of high voltage pulse transformers for klystron modulators 2014 IEEE International Power Modulator and High Voltage Conference (IPMHVC), 2014, pp. 197-200, doi: 10.1109/IPMHVC.2014.7287242

[6] Guillod T. et al.: Artificial Neural Network (ANN) Based Fast and Accurate Inductor Modeling and Design, IEEE open journal of Power Electronics, Vol. 1, pp. 284-299

[7] Arnoux P.-H. et al.: Modeling Finite-Element Constraint to Run an Electrical Machine Design Optimization Using Machine Learning, IEEE Transactions on Magnetics, Vol. 51, no 3, 4 p.

[8] Burrascano P. et al.: Neural Models of Ferrite Inductors Non-Linear Behavior, IEEE International Symposium on Circuits and Systems (ISCAS), 2019, 5 p.

[9] Cincotti S. et al.: A neural network model of parametric nonlinear hysteretic inductors, IEEE Transactions on Magnetics, Vol 34, no 5, 3040-3043

[10] “Pytorch,” PyTorch. [Online]. Available: https://pytorch.org/. [Accessed: 08-Dec-2021].

[11] Bengio, Yoshua; LeCun, Yann; Hinton, Geoffrey (2015). "Deep Learning". Nature. 521 (7553): 436–444. Bibcode:2015Natur.521..436L. doi:10.1038/nature14539. PMID 26017442. S2CID 3074096

[12] “Optuna” [Online]. Available: https://optuna.org/. [Accessed: 08-Dec-2021].

[13] Lasdon L.S. et al.: Design and Testing of a Generalized Reduced Gradient Code for Nonlinear Programming, ACM Transactions on Mathematical SoftwareVolume 4 Issue 1March 1978 pp 34-50. doi:10.1145/355769.355773